Artifact Properties of Dental Ceramic and Titanium Implants in MRI

Artefakt-Verhalten von dentalen Keramik- und Titanimplantaten im MRT

Authors

Margit-Ann Geibel[1], Benjamin Gelißen[2], Anna-Katinka Bracher[3], Volker Rasche[3]

Affiliations

1 Oral and Maxillofacial Surgery, Ulm-University, Ulm Germany
2 Dental Office Benjamin Gelißen, Schwerin, Germany
3 Internal Medicine II, Ulm-University, Ulm, Germany

Key words

peri-implantitis, magnetic resonance imaging, ceramic implant, titanium implant, three-dimensional imaging, artifacts

received 21.12.2017
accepted 19.09.2018

Bibliography

DOI https://doi.org/10.1055/a-0755-2374
Published online: 12.11.2018
Fortschr Röntgenstr 2019; 191: 433–441

ISSN 1438-9029

Correspondence

Prof. Margit-Ann Geibel
Zahnheilkunde, Universität Ulm, Albert-Einstein-Allee 11, 89081 Ulm, Germany
Tel.: ++ 49/7 31/50 06 43 03
Fax: ++ 49/7 31/50 06 43 02
margrit-ann.geibel@uniklinik-ulm.de

ABSTRACT

Aim Assessment of the visualization of titanium and ceramic dental implants using various isotropic three-dimensional magnetic resonance imaging (MRI) methods.

Materials and Methods 21 dental implants (7 ceramic, 14 titanium) were scanned in vitro with a spatially isotropically resolved three-dimensional gradient echo (FFE), a turbo spin echo (SE) and an ultra-short-echo time (UTE) imaging technique. The resulting absolute volumes of the implants were quantified and the relative error to the theoretical volume was calculated.

Results Ceramic implants and their periphery could be displayed well in all cases. The observed mean relative error results were 5.4 ± 2.3 % (UTE) to 6.5 ± 4.3 % (FFE). No significant difference was observed between the investigated MRI methods. The transition between implant and surrounding agarose could be shown in all cases without artifacts. Titanium implants resulted in mean relative errors between 1314 ± 350 % (FFE) and 2157 ± 810 % (SE). Here, significant differences were observed between the FFE and the SE and between the UTE and the SE sequence. The periphery of the implants could not be displayed in any case.

Conclusion Use of the MRI technique for the diagnosis of peri-implantitis, the assessment of anatomical structures and planning of dental implantation is currently very limited but could be used more frequently, provided there are no disturbing or imaging-disturbing materials in the region of interest. MRI technology is not suitable in case of titanium implants. When using ceramic implants, MRI technology is an option.

Key points

- MRI allows the artifact-free depiction of dental ceramic implants.
- Titanium implants cause the greatest relative errors in SE techniques.
- The UTE technique shows no significant improvements with respect to artifact behavior over the FFE technique.

Citation Format

- Geibel M, Gelißen B, Bracher A et al. Artefakt-Verhalten von dentalen Keramik- und Titanimplantaten im MRT. Fortschr Röntgenstr 2019; 191: 433–441

ZUSAMMENFASSUNG

Ziel Untersuchung der Darstellbarkeit von dentalen Titan- und Keramikimplantaten mittels verschiedener, räumlich isotrop aufgelöster 3-dimensionaler magnetresonanztomografischer (MRT) Untersuchungsmethoden.

Material und Methoden 21 dentale Implantate (7 aus Keramik, 14 aus Titan) wurden in vitro mit einer räumlich isotrop aufgelösten 3-dimensionalen Gradientenecho (FFE), einer Turbo-Spinecho (SE) und einer Ultra-Short-Echo-Time (UTE)-Messtechnik gescannt. Die resultierenden absoluten Volumina der Implantate wurden quantifiziert und der relative Fehler zum theoretischen Volumen berechnet.

Ergebnisse Keramikimplantate und deren Peripherie konnten in allen Fällen gut dargestellt werden. Es resultierte ein mittlerer Fehler von 5,4 ± 2,3 % (UTE) bis 6,5 ± 4,3 % (FFE). Es wurde keine signifikante Differenz zwischen den untersuchten Messmethoden beobachtet. Der Übergang zwischen Implantat und umgebender Agarose konnte in allen Fällen Artefakt-frei dargestellt werden. Titanimplantate resultierten in

Fehlern zwischen 1314 ± 350 % (FFE) und 2157 ± 810 % (SE). Hier wurden signifikante Unterschiede zwischen der FFE und der SE und zwischen der UTE und der SE-Sequenz beobachtet. Die Peripherie der Implantate konnte in keinem Fall dargestellt werden.

Schlussfolgerungen Die Anwendung der MRT-Technik zur Diagnostik von Periimplantitis, Beurteilung anatomischer Strukturen und Planung dentaler Implantation ist derzeit sehr limitiert, könnte aber vermehrt genutzt werden, sofern keine störenden oder die Bildgebung störenden Materialien im Bereich der region-of-interest vorhanden sind. Die MRT-Technologie ist für Fragestellungen, die Titanimplantate betreffen, nicht geeignet. Bei Verwendung von Keramikimplantaten ist die MRT-Technologie eine Option.

Introduction

12.4 % of 65 – 74-year-olds have no teeth [1]. Due to the importance of implants for oral rehabilitation after the loss of natural teeth [2], preoperative imaging is required for optimal treatment planning with maximum risk reduction and predictability of long-term success [3, 4]. MRI could play an important role here due to the visualization of soft-tissue structures [5].

The biggest problem with respect implant care is the risk of peri-implant infection. Implant loss [7] is increasingly being seen as a result of the growing prevalence of peri-implantitis [6]. Therefore, early visualization of peri-implant infections is important. The current gold standard for the visualization of implants is based on X-ray methods such as the panoramic radiograph (▶ **Fig. 1a**) and the classic bitewing X-ray (▶ **Fig. 1b, c**).

Although implants can be effectively visualized with these classic methods, relevant information along the direction of projection is lost as a result of the two-dimensional measurement technique. Therefore, studies are increasingly focusing on three-dimensional diagnostic imaging methods [3, 4]. With respect to the prevalence of peri-implant infections and their consequences, the S3 guidelines come to the conclusion that the prevention of peri-implantitis is cheaper than the treatment of the disease. Therefore, the authors of the guidelines feel that three-dimensional imaging (primarily DVT) can be used for the visualization of advanced and complex lesions, for treatment planning and for treatment decisions [8].

However, DVT imaging seems to be problematic with respect to the evaluation of osseointegration. In addition to the radiation exposure for the patient, it is often not possible to evaluate inflammatory processes due to the limited soft-tissue contrast and to visualize the implant interface due to artifacts in the case of both titanium and ceramic implants (▶ **Fig. 2**).

Due to the high-contrast visualization of soft tissues, MRI represents an attractive radiation-free alternative here [4, 5, 9 – 14]. However, the MRI method is limited by its sensitivity to metals and the resulting artifacts [2, 15]. In most cases, titanium implants could not be evaluated, while ceramic implants were artifact-free (▶ **Fig. 3**).

A strong dependence of the resulting artifacts on the dental material and the sequence was observed [14, 16 – 21].

To evaluate the applicability of MRI for visualizing an implant after implantation, various three-dimensional MR measurement sequences (spin echo (SE), gradient echo (GE), ultrashort TE (UTE)) with isotropic spatial resolution were compared with respect to artifacts for titanium and ceramic implants in the present study.

Materials and Methods

Implants

In total, 8 (2 ceramic (#1, #8), 6 titanium (#2 – #7)) different implant types were examined (see ▶ **Table 1**). In three cases, multiple implants (#3: 7; #6: 3; #8: 6) of the same type were examined, with implants from two different lots being included in cases #3 and #8. To achieve conditions that were as realistic as possible, all implants were removed from sterile packaging and sterilized immediately prior to the experiment. Each implant was embedded in agarose (SERVA® tablets (Serva, Heidelberg), 0.5 g/tablet, molecular biology grade) in a sealable transparent specimen container and then examined using the standardized MR protocol.

MR – measurement protocol

All data were recorded on a clinical 3 T whole-body MRI unit (Achieva 3 T, Philips Healthcare, Best, The Netherlands). For the measurement, the embedded implants were fixed to a segment of a 2 × 2-channel carotid coil in random orientation. The measurement protocol included spatially isotropically resolved three-dimensional sequences. A T1-weighted turbo spin echo (SE) sequence and a corresponding steady-state gradient echo (FFE) sequence were used as the clinically established sequences. In addition, an ultrashort TE (UTE) sequence was examined as a special technique for reducing metal-induced signal cancellation [21]. Detailed acquisition parameters are provided in ▶ **Table 2**.

Data analysis

The sequences and implants were compared based on the measured volumes of the implants including signal cancellation in the acquired volume datasets. These were segmented using a region-growing technique semiautomatically via ITK Snap® Version 2.2.0. To facilitate segmentation, seed points were manually set in the region of the implants to support the region-growing algorithm. The various implants and measurement techniques were compared by determining the relative error in comparison to the real implant volumes provided by the manufacturers.

Statistical significance was determined using a two-sided paired student's t-test. Differences with p-values less than 0.05 were considered significant.

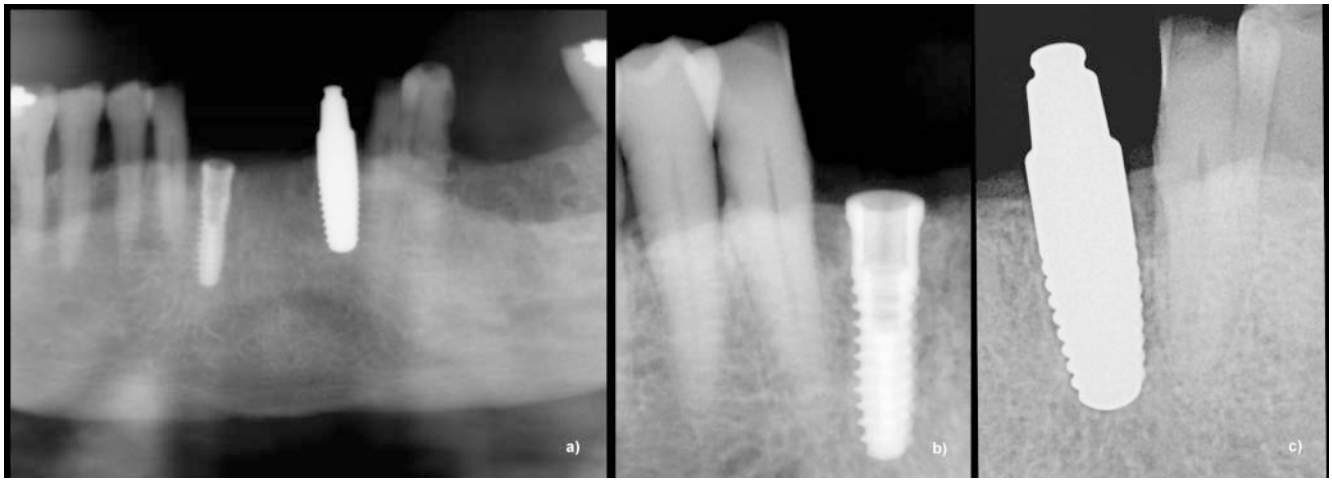

▶ **Fig. 1** OPG **a** and single-tooth radiograph (**b**, **c**) images of a titanium implant in region 42 **b** and for a ceramic implant in region 32 **c**.

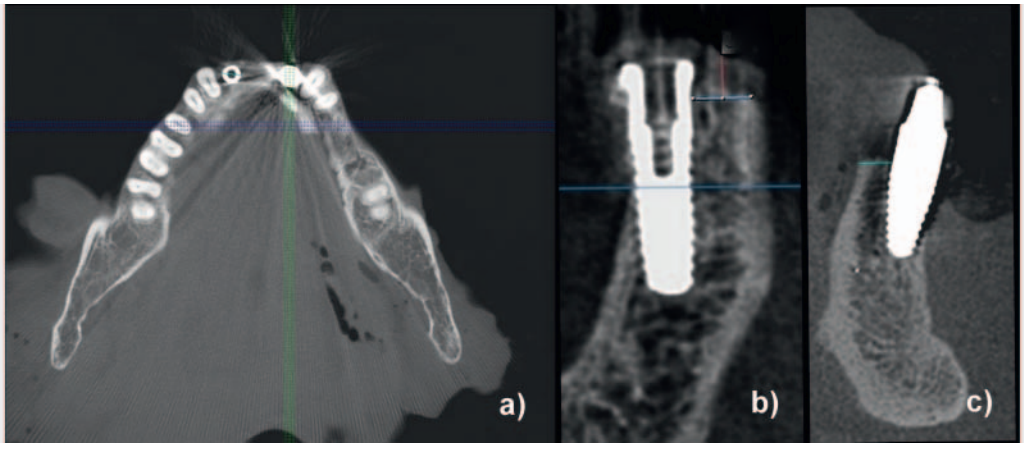

▶ **Fig. 2** CBCT representation of the titanium (42, **b**) and ceramic implant (32, **c**). Please note the severe long-ranging streak artifacts caused by the implants **a**.

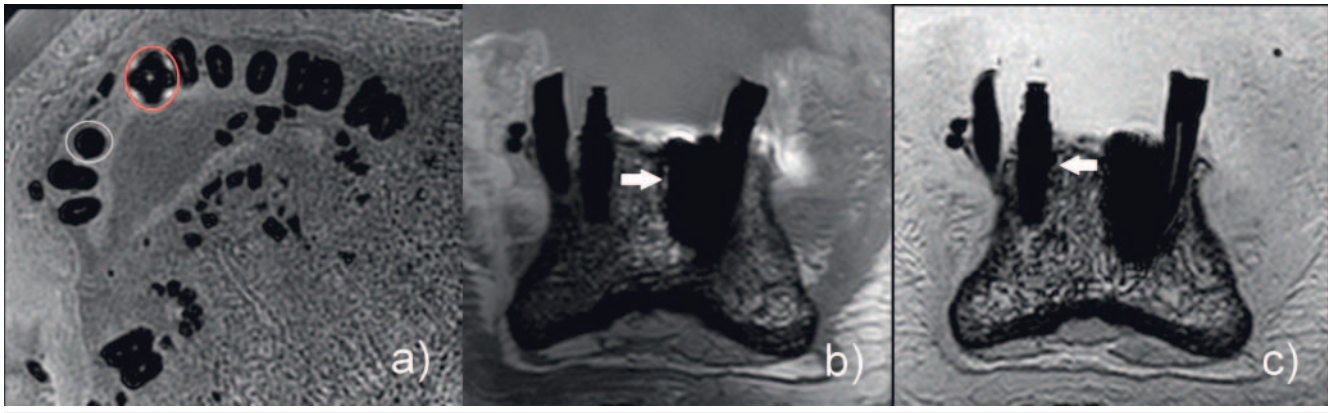

▶ **Fig. 3** MRI representation of the titanium (42, red circle in **a**, arrow in **b**) and ceramic (32, white circle in **a**, arrow in **c**) implant. Please note the only local artifacts caused by the titanium implant and lack of artifacts for the ceramic implant **a**.

▶ **Table 1** Implants (#1 Ziterion, #2 – 8 Bredent).

implant number	model name	implant diameter	implant length
#1	ZI510H®	5.0 mm	10 mm
#2	bSKY4010®	4.0 mm	10 mm
#3 (7 units)	SKY4514®	4.5 mm	14 mm
#4	bSKY4012®	4.0 mm	12 mm
#5	bSKY3514®	3.5 mm	14 mm
#6 (3 units)	SKY4512®	4.5 mm	12 mm
#7	bSKY4510®	4.5 mm	10 mm
#8 (6 units)	white sky SKY4512C®	4.5 mm	12 mm

▶ **Table 2** Summary of the relevant MR parameters.

measurement parameters	UTE	SE	FFE
FOV RL/FH(mm)	120	120	120
AP(mm)	120	30	60
voxel size RL/FH/AP(mm)	0.5	0.5	0.5
TR/TE (ms)	12/0.14 (3 × oversampled)	419/11 (4 echoes)	5.5/2.0
total scan duration	31 m 41 s	25 m 8 s	2 m 38 s
BW (Hz)	656.5	444.6	1883.2

Results

The measurements were successfully performed for all implants. ▶ **Fig. 4** shows an example of the central layer of a titanium and a ceramic implant visualized with the investigated MR techniques.

Significant artifacts and deformations were observed for all titanium implants. Even if a dependence of the resulting artifacts on the orientation of the implant was observed, it was not possible to evaluate the direct periphery of the implants in any of the examined cases. Extensive artifacts, as observed for example in DVT (▶ **Fig. 2a**), were not seen. Artifacts were limited to the immediate vicinity of the implants.

No artifacts were observed in the case of the ceramic implants and the periphery of the implants was also able to be effectively evaluated. Any limitations are the result of the moderate spatial resolution of 0.5^3 mm^3.

The quantitative analysis of the implants is summarized in Tables 3 – 7. The direct comparison of the quantified volumes in the MR data with the theoretical values (titanium, ▶ **Table 3**; ceramic, ▶ **Table 5**) and the resulting relative errors (titanium, ▶ **Table 4**; ceramic, ▶ **Table 6**) highlight the qualitative impression of the images. Regardless of the measurement sequence, an average relative error of more than 1000 % was observed for the titanium implants. Average errors of only 5 % were seen for the ceramic implants. Among the MR measurement sequences, significant differences were seen between FFE and SE ($p < 0.001$) as well as UTE and SE ($p < 0.01$) but not between FFE and UTE ($p = 0.47$) for the titanium implants. No significant differences were seen for the ceramic implants.

The direct comparison between the theoretical implant volume and the MRI measurements is highly significant ($p < 0.001$) for all titanium implants and measurement sequences. Significant differences for FFE ($p < 0.05$) and SE ($p < 0.05$) but not for UTE ($p = 0.06$) were observed for the ceramic implants.

The means and standard deviation of the implants that were investigated multiple times (#3, #6, #8) are shown in ▶ **Table 7**. Significant variation was also seen in the results for the titanium implants that were measured several times. Interestingly, the greatest variations occurred in the SE sequence, while the smallest amount of variation was seen in the FFE sequence.

Discussion

The use of MRI for the three-dimensional visualization of titanium and ceramic implants and the surrounding structures was examined on the basis of various MR sequences. Interestingly, the greatest variation and also the greatest errors for all implant types were seen in the case of the SE technique. UTE and FFE did not show significant differences. Significant differences were only observed in the case of the titanium implants. This is most likely due to the strong magnetic field interference caused by the titanium

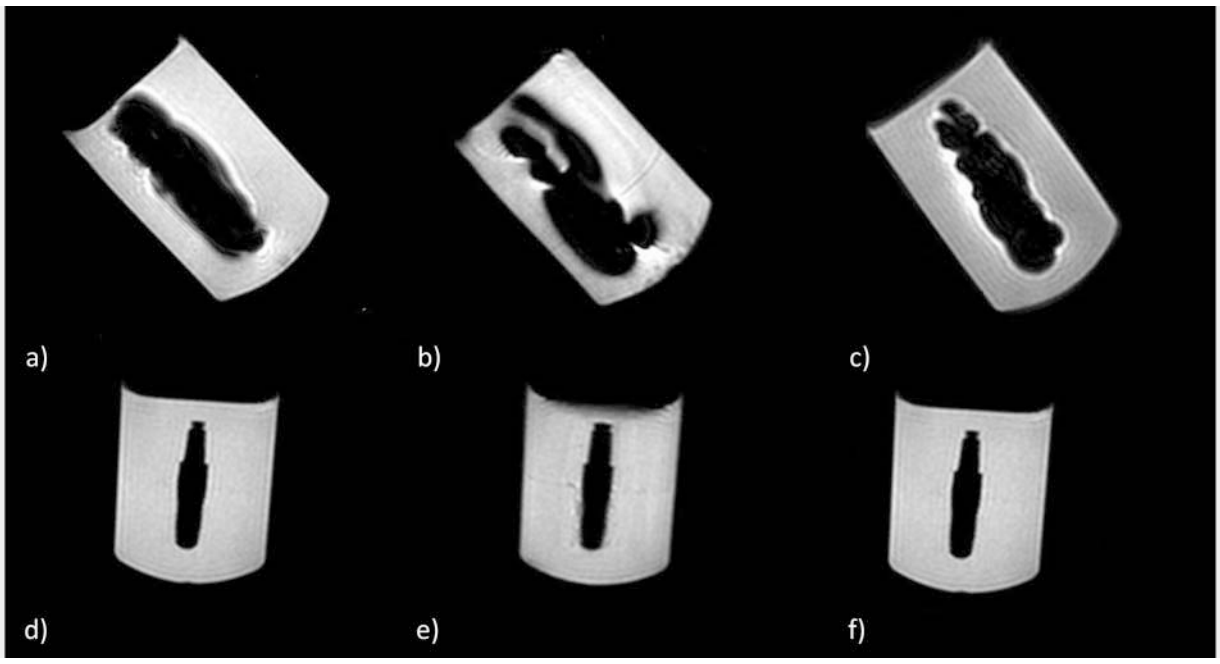

▶ **Fig. 4** MRI representation of a titanium (#6, **a – c**) and ceramic (#1, **d – f**) implant acquired with FFE (**a**, **d**), SE (**b**, **e**) and UTE (**c**, **f**).

▶ **Table 3** Theoretical (actual vol.) and measured (digital vol.) volume for titanium implants resulting from the investigated MR sequences.

impl. no.	actual vol. [mm³]	digital vol. FFE [mm³]	digital vol. SE [mm³]	digital vol. UTE [mm³]
#2	76.39	977.62	1412.27	878.95
#3A_1.Ch	143.73	1840.74	2884.66	1244.22
#3B_1.Ch	143.73	1846.15	4066.83	2620.81
#3C_1.Ch	143.73	2166.51	4200.02	3116.91
#3A_2.Ch	143.73	1628.85	2564.22	2506.02
#3B_2.Ch	143.73	1903.43	2576.62	1294.79
#3C_2.Ch	143.73	2646.00	4790.89	2744.59
#3D_3.Ch	143.73	1706.86	1894.40	2447.09
#4	90.91	1039.95	1354.20	1134.07
#5	80.53	880.08	1210.67	763.50
#6A	122.23	2506.31	2086.87	1638.13
#6B	122.23	2271.29	4327.23	3438.55
#6C	122.23	2281.90	4416.76	1707.26
#7	102.28	976.27	1960.93	989.12

implants, which, in connection with the low bandwidth of the excitation and refocusing pulses of the SE sequence, allows only incomplete excitation of the surrounding tissue.

The minimal standard deviation of the ceramic implant results (FFE: 6.5 ± 4.3 %; SE: 6.4 ± 2 %; UTE: 5.3 ± 2.3 %) indicates position and orientation independence of this implant type. In the case of titanium implants, a strong dependence of the artifacts on implant position and particularly orientation was observed as shown by the significant variability of the results (FFE: 1766 ± 348 %; SE: 2157 ± 810 %; UTE: 1398 ± 562 %).

As expected and also proven by other studies [11, 13, 15, 22, 23], all titanium implants caused artifacts, some of which were quite significant, thereby rendering evaluation of the implant shape and the structures near the implant impossible. Therefore, the MRI technique currently cannot be used as an alternative to conventional imaging methods in the region of titanium implants. However, ceramic implants and the immediate vicinity can be visualized clearly and pre-

▶ **Table 4** Relative error for titanium implants resulting from the investigated MR sequences.

impl. no.	error FFE [%]	error SE [%]	error UTE [%]	average error (standard deviation) [%]
#2	1179.85	1748.86	1050.67	1326 (371)
#3A_1.Ch	1180.71	1907.03	765.68	1285 (578)
#3B_1.Ch	1184.48	2729.53	1723.45	1879 (784)
#3C_1.Ch	1407.36	2822.20	2068.62	2099 (707)
#3A_2.Ch	1033.29	1684.08	1643.59	1454 (363)
#3B_2.Ch	1224.33	1692.71	800.86	1239 (446)
#3C_2.Ch	1740.98	3233.30	1809.58	2261 (842)
#3D_3.Ch	1087.56	1218.05	1602.58	1302 (267)
#4	1043.88	1389.54	1147.41	1194 (177)
#5	992.90	1403.43	848.13	1081 (288)
#6A	1950.44	1607.29	1240.17	1599 (355)
#6B	1758.16	3440.15	2713.11	2637 (844)
#6C	1766.84	3513.40	1296.73	2193 (1167)
#7	854.54	1817.28	867.10	1179 (552)

▶ **Table 5** Theoretical (actual vol.) and measured (digital vol.) volume for ceramic implants resulting from the investigated MR sequences.

impl. no.	actual vol. [mm³]	digital vol. FFE [mm³]	digital vol. SE [mm³]	digital vol. UTE [mm³]
#1	221.93	249.20	242.19	237.30
#8A_1.Ch	239.69	258.75	247.72	256.14
#8B_1.Ch	239.69	247.60	252.07	257.73
#8C_1.Ch	239.69	257.88	257.86	225.75
#8A_2.Ch	239.69	243.35	226.64	258.86
#8B_2.Ch	239.69	272.93	256.67	255.32
#8C_2.Ch	239.69	251.51	257.97	242.95

▶ **Table 6** Relative error for ceramic implants resulting from the investigated MR sequences.

impl. no.	error FFE [%]	error SE [%]	error UTE [%]	average error (standard deviation) [%]
#1	12.29	9.13	6.92	9.4 (2.7)
#8A_1.Ch	7.95	3.35	6.86	6.1 (2.4)
#8B_1.Ch	3.30	5.17	4.72	4.4 (1.0)
#8C_1.Ch	7.59	7.58	5.81	7.0 (1.0)
#8A_2.Ch	1.53	5.45	8.00	5.0 (3.3)
#8B_2.Ch	10.89	7.09	3.74	7.2 (3.6)
#8C_2.Ch	2.03	7.63	1.36	3.7 (3.4)

▶ **Table 7** Mean and standard deviation (in parentheses) of the volume and relative error for the titanium (#3, #6) and ceramic (#8) implant series.

means	#3	#6	#8
volume FFE [mm^3]	1962 (345)	2532 (132)	255 (10)
volume SE [mm^3]	3282 (1067)	3610 (1320)	249 (12)
vol. UTE [mm^3]	2282 (725)	2261 (1012)	249 (12)
error FFE [%]	1265 (855)	1825 (108)	5.6 (3.8)
error SE [%]	2183 (1817)	2853 (1080)	6.0 (1.7)
error UTE [%]	1487 (867)	1750 (867)	5.1 (2.4)

cisely so that MRI can be considered as an alternative method for monitoring the healing process of ceramic implants.

Currently available data

Diagnostic imaging is important for reducing implant risks [24 – 26]. The use of OPG for preoperative planning and postoperative assessment of standard titanium implants currently represents the clinical standard [27]. In contrast to other disciplines [3, 4, 10 – 12, 28], the use of MRI is limited in dentistry due to the susceptibility to metal-induced artifacts [11, 14, 19]. Metal objects cause artifacts and image distortion in MRI [11, 13, 15, 22]. The resulting artifacts vary based one differences in the susceptibility of the materials being used, the shape and orientation of the object, the material composition, and the magnetic field strength [10, 11, 14, 22, 29, 30].

Although titanium dental implants have been classified as biocompatible for many years and represent the gold standard in dental implantology due to their positive material properties [13, 31 – 33], ceramic implants have been having a renaissance in recent years [20, 23, 34, 35]. Various studies have proven excellent osseointegration, high biocompatibility, and a positive tissue response [35 – 39]. Moreover, studies have shown a connection between titanium implants and allergic reactions, inflammation, hematological and metabolic toxicity and hypersensitivities to metal components [35 – 37, 39]. The new generation of ceramic implants offers new possibilities in the field of implantology.

In an in vitro study, Duttenhofer et al. compared MRI vs. conventional X-ray methods (OPG, DVT and CT) for examining titanium and ceramic implants in order to evaluate the accuracy of the methods for preimplant planning and postoperative follow-ups [27]. They were able to show that the quality of preoperative imaging was the same for all methods. However, significant image distortion in postoperative imaging was seen in the case of titanium implants in contrast to ceramic implants.

Matsuura et al. examined 6 different types of ceramic, pure titanium, and titanium alloys for susceptibility artifacts. The results confirmed the conclusion of other studies that all tested ceramics resulted in much less significant artifacts than the examined metals [40]. They concluded that ceramic is the biomaterial that is best suited for reducing artifacts when using MRI [40].

This study confirmed that titanium implants cause major artifacts in every examined measurement technique [11, 13, 15, 31], while the images of all examined ceramic implants were artifact-free. Therefore, it can thus be assumed that ceramic implants can be visualized in precise detail with MRI. Thus, MRI can be used as an alternative to the gold standard, X-ray imaging, as long as there are no metal objects in the immediate vicinity [27].

Clinical significance

The investigated MRI methods cannot be used to evaluate the periphery of titanium implants. However, the results show that ceramic implants can be precisely visualized with various MRI methods. It can be assumed that MRI can play an increasingly relevant role in the evaluation of implantation results as well as the evaluation of the healing process and the diagnosis of peri-implant complications at least in the case of ceramic implants.

Limitations

The effect of the position and orientation of the implant relative to the direction of the static magnetic field was not systematically examined. However, a significant relationship between titanium implant-induced artifacts and implant orientation can be concluded from the observed variability of the results.

The evaluation method used in this study did not include analysis of possible distortions and it is theoretically possible for distortion of the examined implant with the same volume to occur. This was not observed in the visual assessment of the results but may require further study.

Moreover, the measurement sequences used in this study are not sequences used in the clinical routine. Undersampling (parallel imaging, compressed sensing) was not used to accelerate the process and the geometric isotropic coverage of the measurement volume resulted in unacceptable measurement times for the clinical routine in particular for the spin echo and UTE techniques.

Conclusion

The results of this study showed that MRI technology could be an alternative to conventional radiology, CT and DVT for the evaluation of ceramic implants since, in contrast to titanium implants, both the ceramic implant and the peri-implant region can be effectively visualized in vitro with MRI. Thus, it is possible to obtain relevant information for diagnosis and treatment decisions in the case of peri-implant complications without radiation exposure

and with improved visualization of the surrounding soft tissue via the three-dimensional visualization of the implant periphery.

Conflict of Interest

The authors declare that they have no conflict of interest.

References

[1] Jordan AR, Micheelis W. Fünfte Deutsche Mundgesundheitsstudie (DMS V). Materialienreihe Bd. 35, Institut der Deutschen Zahnärzte (Hrsg.), Köln: Deutscher Zahnärzte Verlag DÄV; 2016

[2] Schwenzer N, Ehrenfeld M. Chirurgische Grundlagen. 4. Aufl Stuttgart: Thieme; 2008: 118 – 165. doi:10.1055/b-00000021

[3] Scherer P, Neugebauer J, Ritter L et al. Indikationen für die 3-dimensionale Bildgebung in der Zahnheilkunde. ZWR 2007; 116: 219 – 230. doi:10.1055/s-2007-983917

[4] Schulze R. DVT-Diagnostik in der Implantologie: Grundlagen-Fallstricke. ZMK Zahnheilkunde, Management, Kultur (15.02.2011). Im Internet: https://www.zmk-aktuell.de/fachgebiete/implantologie/story/dvt-diagnostik-in-der-implantologie-grundlagen–fallstricke__404.html. Stand: 03.02.2017

[5] Geibel MA, Schreiber E, Bracher AK et al. Characterisation of apical bone lesions: Comparison of MRI and CBCT with histological findings – a case series. Eur J Oral Implantol 2017; 10: 197 – 211

[6] Schwarz F, Becker J. Periimplantäre Infektionen – Ein Update zur Epidemiologie, Ätiologie, Diagnostik, Prävention und Therapie. Implantologie 2015; 23: 247 – 259

[7] Mombelli A, Lang NP. (1998). The diagnosis and treatment of peri-implantitis. Periodontology 2000; 17: 63 – 76. doi:10.1111/j.1600-0757.1998.tb00124.x

[8] Schwarz F, Becker J. Die Behandlung periimplantärer Infektionen an Zahnimplantaten. S3-Leitlinie (Langversion). AWMF-Registernr. 083-023. 2016: 5 – 14

[9] Geibel MA, Schreiber ES, Bracher AK et al. Assessment of apical periodontitis by MRI: a feasibility study. Rofo 2015; Apr 187: 269 – 275

[10] Abbaszadeh K, Heffez LB, Mafee MF. Effect of interference of metallic objects on interpretation of T1-weighted magnetic resonance images in the maxillofacial region. Oral Surg Oral Med Oral Pathol Oral Radiol Endod 2000; 89: 759 – 765

[11] Costa AL, Appenzeller S, Yasuda CL et al. Artifacts in brain magnetic resonance imaging due to metallic dental objects. Medicina Oral Patologia Oral Y Cirugia Bucal 2009; 14: 278 – 282

[12] Gray CF, Redpath TW, Smith FW et al. Advanced imaging: Magnetic resonance imaging in implant dentistry. Clin Oral Implants Res 2003; 14: 18 – 27. doi:10.1034/j.1600-0501.2003.140103.x

[13] Harris TMJ, Faridrad MR, Dickson JAS. The Benefits of Aesthetic Orthodontic Brackets in Patients Requiring Multiple MRI Scanning. J Orthod 2006; 33: 90 – 94. doi: 10.1179/146531205225021465

[14] Hilgenfeld T, Prager M, Schwindling FS et al. Artefacts of implant-supported single crowns – Impact of material composition on artefact volume on dental MRI. Eur J Oral Implantol 2016; 3: 301 – 308

[15] Shafiei F, Honda E, Takahashi H et al. Artifacts from Dental Casting Alloys in Magnetic Resonance Imaging. J Dent Res 2003; 82: 602 – 606. doi: 10.1177/154405910308200806

[16] Cortes AR, Abdala-Junior R, Weber M et al. Influence of pulse sequence parameters at 1.5 T and 3.0 T on MRI artefacts produced by metal-ceramic restorations. Dentomaxillofac Radiol 2015; 44: 20150136. doi: 10.1259/dmfr.20150136. Epub 2015 Jun 18. PubMed PMID: 26084475; PubMed Central PMCID: PMC4628425

[17] Burchardt DV, Borysewicz-Lewicka M. Disturbing effect of different dental materials on the MRI results: preliminary study. Acta Bioeng Biomech 2013; 15: 49 – 55. PubMed PMID: 24479695

[18] Tymofiyeva O, Vaegler S, Rottner K et al. Influence of dental materials on dental MRI. Dentomaxillofac Radiol 2013; 42: 20120271. doi: 10.1259/dmfr.20120271. Epub 2013 Apr 22. PubMed PMID: 23610088; PubMed Central PMCID: PMC3667526

[19] Eggers G, Rieker M, Kress B et al. Artefacts in magnetic resonance imaging caused by dental material. Magnetic Resonance Materials in Physics, Biology and Medicine/MAGMA 2005; 18: 103 – 111. doi:10.1007/s10334-005-0101-0

[20] Suh JS, Jeong EK, Shin KH et al. Minimizing artifacts caused by metallic implants at MR imaging: experimental and clinical studies. Am J Roentgenol 1998; 171: 1207 – 1213. doi:10.2214/ajr.171.5.9798849

[21] Bracher AK, Hofmann C, Bornstedt A et al. Ultrashort echo time (UTE) MRI for the assessment of caries lesions. Dentomaxillofac Radiol 2013; 42: 20120321. doi: 10.1259/dmfr.20120321. Epub 2013 Feb 18

[22] Shellock FG, Kanal E, Yasargil ■. Aneurysm clips: evaluation of interactions with a 1.5-T MR system. Radiol 1998; 207: 587 – 591. doi:10.1148/radiology.207.3.9609877

[23] Wang W, Jiang B, Wu X et al. Influences of three types of dental ceramic alloys on magnetic resonance imaging. Zhongguo Yi Xue Ke Xue Yuan Xue Bao 2010; 32: 276 – 279. doi:10.3881/j.issn.1000-503X.2010.03.008

[24] Köhler SG. Risiken, Fehler und Komplikationen. Implantologie 2008; 32: 12 – 18

[25] Hassfeld S, Streib S, Sahl H et al. Low-dose-Computertomografie des Kieferknochens in der präimplantologischen Diagnostik. Mund Kiefer Gesichts Chir 1998; 2: 188 – 193. doi:10.1007/s100060050057

[26] Brüllmann D, Schulze R. Zukünftige Entwicklungen in der digitalen dentalen Volumentomografie–Teil 2. Apollonia, 2011. 12: 00

[27] Duttenhoefer F, Mertens ME, Vizkelety J et al. Magnetic resonance imaging in zirconia-based dental implantology. Clin Oral Implants Res 2014; 00: 1 – 8. doi: 10.1111/clr.12430

[28] Schulze R. Aktueller Stand der digitalen Röntgentechnik. ZM 2006; 96: 42

[29] Cortes AR, Abdala-Junior R, Weber M et al. Influence of pulse-sequence parameters at 1. 5 T and 3.0 T on MRI artefacts produced by metal-ceramic restorations. Dentomaxillofac. Radiol 2015; 44: 20150136. doi: 10.1259/dmfr.20150136

[30] Xu Y, Yu R. Comparison of magnetic resonance imaging artifacts of five common dental materials. Hua xi kou Qiang yi xue za zhi 2015; 33: 230 – 233

[31] Idiyatullin D, Corum C, Moeller S et al. Dental Magnetic Resonance Imaging: Making the Invisible Visible. J Endod 2011; 37: 745 – 752. doi: 10.1016/j.joen.2011.02.022

[32] Hubálková H, Hora K, Seidl Z et al. Dental materials and magnetic resonance imaging. Eur J Prosthodont Restor Dent 2002; 10: 125 – 130

[33] Tutton L, Goddard P. MRI of the teeth. Br J Radiol 2002; 75: 552 – 562. doi: 10.1259/bjr.75.894.750552

[34] Siddiqi A, Payne AGT, De Silva RK et al. Titanium allergy: could it affect dental implant integration. Clin Oral Implants Res 2011; 22: 673 – 680. doi:10.1111/j.1600-0501.2010.02081.x

[35] Assal P. The Osseointegration of Zirconia Dental Implants. Schweiz Monatsschr Zahnmed 2012; 123: 644 – 654

[36] Hisbergues M, Vendeville S, Vendeville P. Zirconia. Established facts and perspectives for a biomaterial in dental implantology. J Biomed Mater Res B Appl Biomater 2009; 88: 519 – 529. doi:10.1002/jbm.b.31147

[37] Hoffmann O, Angelov N, Zafiropoulos G et al. Osseointegration of zirconia implants with different surface characteristics: an evaluation in rabbits. Int J Oral Maxillofac Implants 2012; 27: 352 – 358

[38] Muddugangadhar BC, Amarnath GS, Tripathi S et al. Biomaterials for dental implants: An overview. Intern J Oral Impl Clin Res 2011; 2: 13 – 24

[39] Stadlinger B, Hennig M, Eckelt U et al. Comparison of zirconia and titanium implants after a short healing period. A pilot study in minipigs. Int J Oral Maxillofac Surg 2010; 39: 585 – 592. doi:10.1016/j.ijom.2010.01.015

[40] Matsuura H, Inoue T, Konno H et al. Quantification of susceptibility artifacts produced on high-field magnetic resonance images by various biomaterials used for neurosurgical implants. J Neurosurg 2002; 97: 1472 – 1475. doi: 10.3171/jns.2002.97.6.1472